JCAMECH

Vol. 49, No. 1, June 2018, pp 171-178
DOI: 10.22059/jcamech.2017.238724.170

Surface hardness improvement in high efficiency deep grinding process by optimization of operating parameters

*Hamid Reza Fazli Shahri[1, 2, *], Ali Akbar Akbari[3], Ramezanali Mahdavinejad[1], Ali Solati[1]*

[1]*School of mechanical engineering, College of Engineering, University of Tehran, Tehran, Iran*
[2]*SPGC, Boushehr, Iran*
[3]*Department of mechanical engineering, Faculty of Engineering, Ferdowsi University of Mashhad, Mashhad, Iran*

ARTICLE INFO

Article history:
Received: 01 August 2017
Accepted: 17 October 2017

Keywords:
High efficiency deep grinding
Microhardness
Microstructure
Optimization

ABSTRACT

The grinding is one of the most important methods that directly affects tolerances in dimensions, quality and finished surface of products. One of the major problems in the material removal processes specially grinding is the heat generation during the process and the residual tensile stress in the surfaces of product. Therefore, optimization of High Efficiency Deep Grinding (HEDG) process is the main goal of this study to reduce the generated heat and residual tensile stress and increase strength and surface hardness of AISI1045annealed steel. To this end, the effects of main parameters e.g. depth of cut, wheel speed, workpiece speed and cross feed on surface hardness has been investigated. The experimental results demonstrated the reduction in surface temperature and increase in hardness as optimum conditions are applied to the grinding process. Moreover, the experimental results were validated by comparing with other experimental results and analyzing of surface microhardness, surface temperature and normal and tangential forces.

1. Introduction

Grinding is one of the most important methods that directly affects tolerances in dimensions, quality and finished surface of products. HEDG process has been recently more regarded due to the high rate of wheel speed, depth of cut and cross feed simultaneously. Whereas Low Stress Grinding process (LSG) is applied on products that are often subjected to high stress and corrosive environments, even so, using this method not only residual tensile stresses are not remained on the surface but compressive residual stresses are produced. These products can be employed in dynamic environments. Residual tensile stresses and cracks on surface which corresponded to the heat are some challenges related to grinding [1, 2]. The main source of residual stresses is plastic deformation itself is generally compressive, but thermal stresses often lead to tensile residual stresses. The residual stress induced by the grinding force. The level of the latter is usually much greater than that of the former. Therefore, the residual stress brought about by a grinding operation is generally a tensile stress. In order to limit surface damage and reduce the residual stress, several methods have been proposed, such as heat treatment, lapping, shot peening, and so on. However, there are some shortcomings when using these treatments: (i) an additional process is necessary; and (ii) expensive equipment is required for the treatment. The tensile stress can be reduced to an acceptable level or even converted into a compressive stress, under certain conditions. This possibility has been confirmed by the results of several grinding experiments [3, 4]. The present paper aims to suggest a grinding method of the reduction of surface residual tensile stress by appropriate selection of process parameters. In the area of research where analytical tools are not strong enough to present a reasonable solution to the problem of metal cutting, the optimization method seems more promising.

Because very expensive computer numerical control (CNC) grinding machines and expensive equipment is needed for the shop floor, optimization of grinding conditions has increasingly become important. Selection of grinding parameters is traditionally carried out by process planners either on the basis of their experience on the shop floor or with the help of the data handbooks. Optimization of grinding processes is still as one of the most challenging problems because of its high complexity and non-linearity. Recently, many researchers have tried to demonstrate the potential application of Genetic Algorithm and Tabu Search for single stage optimization problems. However, the application of simulated annealing (SA) in the case of HEDG process optimization problems has not been investigated thoroughly yet. In addition, SA is capable of optimizing a process with a minimum amount of converging time [5]. Therefore, in this study, an optimizing method has been carried out to

[*]Corresponding author. Tel.: +98 912 444 8429; Fax: +98 773131 3280
e-mail: hamidrezafazli65@gmail.com

minimize residual tensile stress and increase surface hardness upon AISI1045 steel. This paper describes SA method (Simulated Annealing) based on optimization procedure to optimize grinding conditions, viz. wheel speed, workpiece speed, depth of cut, cross feed, using a multi-objective function model with a weighted approach. A fully described procedure of this method is in ref. [6]. The procedure evaluates the optimal grinding conditions subjected to constraints such as heat generation, needed forces and surface roughness. Initially a detailed description of the mathematical model of the grinding process is given. Then the optimization procedure is described.

In this study, the obtained resulted from optimization procedure has been tested experimentally then the microhardness values are recorded. These values demonstrate a dramatic increase in hardness from inner sections of material to the surface. The changes in hardness and mechanical properties due to the grinding process have also been studied. One way to investigate residual stress is based on hardness studies which has been performed by Sines and Carlson [7]. Hardness values can be determined by metallographic observation and microhardness measurement. Microhardness, measured along the section of the workpiece, shows marked variations in hardness in the material due to the violent heating and cooling of the surface, and the creation of residual stresses through grinding [7]. Also the surface roughness, surface temperature and grinding forces have to be controlled by adjusting the cutting parameters of the grinding. In brief, this paper studies the superficial changes in the hardness of a workpiece caused by the grinding of AISI 1045 steel, taking into consideration the various parameters that can be controlled in the process; depth of cut, workpiece speed, wheel speed and cross feed.

2. Optimization of operating process parameters

Whereas one of the purposes of this study is mechanical properties improvement in products, the optimization results are very important and should cause to induce hardness and compressive stress at the surface of the workpiece. One of the most considerable challenges upon optimization method is interactions between parameters. In other words, optimization of one special parameter may undesirably affect the others [8, 9]. Hence, a multi-objective SA optimizing algorithm was suggested to satisfy process conditions in which different aspects of grinding process e.g. temperature, hardness, force and roughness were taken into account. Despite the fact that parameters selected by practice and trial-error methods will mostly be on the conservative side and these methods are not reasonable economically, the HEDG process is a very expensive method. Thus, recently there has been interest in determining of optimal machining parameters based on low cost methods, like mathematical and numerical modeling. Optimization analysis of grinding process are usually based on either minimizing needed forces, heat generation, maximizing surface hardness, or obtaining the fitness possible surface roughness by using empirical relationships between the operating parameters. Fortunately, many researchers have published a number of such equations for the practical HEDG process in which numerous process variables are involved. The development of comprehensive grinding process models and computer aided manufacturing provides a basis for realizing grinding parameter optimization. The optimization procedure was performed by SA optimizing algorithm through the toolbox of MATLAB software after determining the mathematical model. A quadratic programming for the optimization of grinding parameters subject to multi-objective function has been used.

3. Mathematical modeling of HEDG process

3.1. Determination of objective function

3.1.1. Hardness sub-objective function

Different mathematical setups have been investigated to produce a reasonable mathematical expression which is a reliable representative of hardness variations. Hardness is presented as a function of various cutting parameters. An expression that authentically declares experimental data for AISI1045 steel is expressed as follows [10]:

$$HB = a_e^{0.0354}\, e^{(4.38+83.7a_e+2.62s-1.07v_w-187s+76.3a_e v_w)} \quad (1)$$

where a_e , v_w and s are depth of cut, workpiece speed and cross feed respectively. This formula was selected among several expressions which were declaration of hardness, because it had a low variance and represented that is in accordance with experimental data.

3.1.2. Heat loading sub-objective function

In according to Werner theory, in deep grinding with a low workpiece speed, the maximum temperature in a zone beneath the new surface of the workpiece can be estimated by the following equation [11]:

$$T_{\max} = \frac{K_T}{0.9}.(v_c)^{0.2}.(a_e v_w)^{0.2}.(a_e)^{(-0.7)}.(d_s)^{0.1} \quad (2)$$

where v_c = wheel speed, d_s = wheel diameter and K_T depends on the process conditions and its range is considered approximately 45-50 in this case based on the experiments.

3.1.3. Mechanical loading sub-objective function

In according to Werner theory, a relation which represents total grinding force with regard to wheel width unit can be estimated by the following equation [11]:

$$F' = \frac{K_n}{0.9}.(\frac{a_e v_w}{v_c})^{0.8}.(a_e d_s)^{0.1} \quad (3)$$

where K_n depends on the process conditions and its range is considered approximately 20-25 in this case. Note that the maximum values for both K_T and K_n are used in optimization procedure.

3.1.4. Surface roughness sub-objective function

The following expression is an approximate formula for surface roughness with regard to cutting parameters. is the maximum variation between the height of tip and depth of valley in a sample length of the workpiece [12] as follows:

$$R_t = (\frac{v_w}{v_c}.\frac{1}{C.r.\sqrt{d_e}})^{(2/3)} \quad (4)$$

where r and C are grit cutting point shape factor and active grit density respectively.

3.1.5. Total objective function

Based on the presented previous functions, the total objective function satisfying all of the considered states can be expressed as sum of the squared errors [5]:

$$EF = W_1 \cdot \frac{(HB^d - HB)^2}{HB^2} + W_2 \cdot \frac{(T_{\max}{}^d - T_{\max})^2}{T_{\max}{}^2} + W_3 \cdot \frac{(F'^d - F')^2}{F'^2} + W_4 \cdot \frac{(R_t{}^d - R_t)^2}{R_t{}^2} \quad (5)$$

Minimizing this function is aimed here where W_i is weighting factor and $\sum_{i=1}^{4} W_i = 1 \rightarrow (0 \le W_i \le 1)$. Index d is representative of the desired value for each parameter as follows:

$$\text{Desired value for each parameter}: \begin{cases} HB^d = 290B \\ T_{\max}{}^d = 450^{\circ}C \\ F'^d = 80N \\ R_t{}^d = 0.5\mu m \end{cases}$$

3.1.6. Process constraints

It is obvious that considering several realistic constraints of the actual HEDG operation is a complete solution to the grinding problems. These constraints can be divided to process constraints and variable constraints. In this work, thermal damages, mechanical loading and surface roughness are considered as process constraints and upper and lower limits of grinding conditions as variable constraints. In some problems with boundary constraints, the value of parameters needs to be within an allowance limit and in this study, the variable constraints determine the upper and lower limits of the grinding conditions.

$$ProcessConstraints: \begin{cases} T_{\max} \le T_{\max}{}^c, T_{\max}{}^c = 550^{\circ}C \\ F' \le F'^c, F'^c = 250N \\ R_t \le R_t^c, R_t^c = 4.5\mu m \end{cases}$$

$$\& \quad VariableConstraints: \begin{cases} 0.005 \le a_e \le 1.5 \\ 0.5 \le v_w \le 30 \\ 5 \le v_c \le 140 \\ 0.05 \le s \le 20 \end{cases}$$

where index *c* is representative of the critical value for each parameter.

3.2. Optimization approach

Traditional approaches are not suitable for a high amplitude optimization problem which has a vast search space. In addition, traditional techniques may be inappropriate for optimizing problems with numerous constraints like several experiments in mass production. The complexity of a special problem may be further increased due to the combinatorial explosion of constraints as the number of stages increases. Therefore, it may be a difficult task for researchers or practitioners to determine a suitable solution procedure for such problems. Hereafter, the full description of Simulated Annealing is provided.

3.2.1. Simulated Annealing algorithm

SA method (Figure 1) is based on a concept of modeling and simulation of a thermodynamic system. Two fundamental operators i.e. neighborhood generation, and cooling schedule function are discussed below.

3.2.2. Neighborhood generation

In this procedure, a new trial point, *x´*, is generated from a current trial point, *x*, based on the following equation:

$$x' = x + \theta(T) \quad (6)$$

and $\theta(T)=T/a$, where a is a scale parameter and *T* is the current value of temperature control parameter which is determined from the cooling schedule function [6].

3.2.3. Cooling schedule

Different cooling schedule functions have been implied and recommended in previous researchers [5]. The cooling schedule purposed in this study is expressed as:

$$T = T_0 (T_n / T_0)^{(t/a)} \quad (7)$$

where T_0, T_n, t, and a are initial temperature, final temperature, counter of temperature changing and scale factor respectively. SA method may also accept inferior state space to generate new neighborhood state space based on an acceptant probability measure. This method avoids trapping in local optimal. The acceptant probability recommended in this study is based on the following formula:

$$Prob\ (acceptance\ of\ an\ inappropriate\ move) = e^{(-\Delta E \beta / T)} \quad (8)$$

where β is a positive number to scale parameter, and ΔE is the changes between two adjacent solutions [5]. SA algorithm was repeated three times for each function.

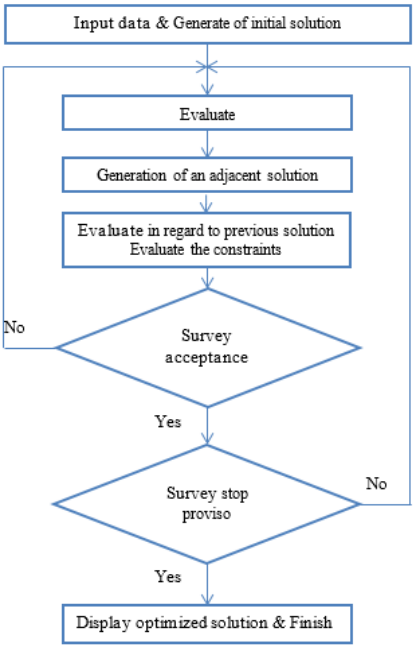

Fig. 1 SA flowchart

4. Experimental procedure

As mentioned before, this work briefly represents the influence of cutting parameters i.e. depth of cut, wheel speed, cross feed and workpiece speed, on the surface hardening of AISI1045 steel during HEDG process. Besides, microstructural changes in the workpiece was also investigated. Although remarkable microstructural changes and phase transformation was not observed within the evaluated states, there was a noticeable change in microhardness as demonstrated in Figure 5. Hence, microhardness and mechanical properties variation caused by

HEDG process were also focused in more detail in this study. The microhardness values measured within a specific section of the workpiece, demonstrated a significant increase. The most common changes are phase transformation, residual stress generation and plastic deformation that eventuate to changes in behavior of the applied materials. During the optimization procedure, the surface roughness, grinding forces and temperature were all controlled by adjusting the cutting parameters of HEDG as well as surface hardness.

The material used in this study was AISI1045 steel, with the chemical composition given in Table 1, which was ground with determined operating parameters in the presence of sufficient water-soluble oil coolant. The workpiece dimensions were $40\times30\times10$ mm^3. The values of operating parameters obtained by optimization procedure were conducted in grinding process and the optimized condition was applied three times on three different samples. Figure 2 illustrates the experimental setup used in this work.

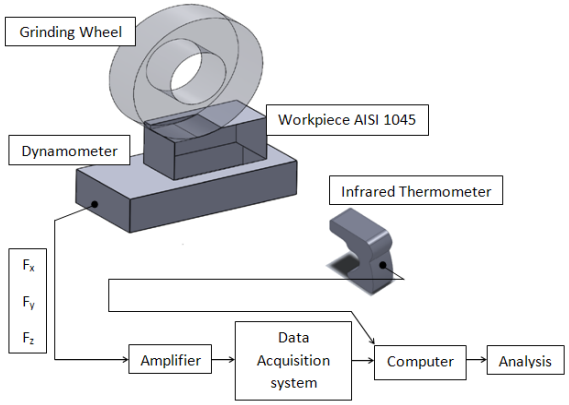

Fig. 2 Experimental setups

4.1. Preparation of Samples (Heat treatment procedure)

All of the samples were subjected to annealing heat treatment. They were kept in the furnace for 1h and 30min at 860°C, in order to achieve a ferrite-pearlite structure as well as lower hardness values which are the result of crystallographic recovery of the material. Subsequently, for cooling the samples they were left in the furnace to reach to the room temperature. As a particular crystallographic orientation of microstructural phases may affect the hardness values, the hardness measuring procedure was performed based on Vickers hardness in a specific traverse section of the workpiece [13].

4.2. HEDG process

A horizontal-spindle machine, with a CBN grinding wheel, with 15mm thickness was employed for grinding the samples. Wheel speed was adjusted with considering different external diameters of grinding wheel. Before each experiment, the external surface of the wheel was dressed by a diamond tip to assure that it's in the best condition. In fact, with very sharp cutting edges, equal conditions for all the experiments were guaranteed.

4.3. Preparation of metallographic samples

In order to study the results of the process more precisely, the microstructure of the samples beneath the ground surface was considered for metallographic analysis. The samples were cut perpendicular to the grinding plane. The metallographic studies were performed according to ASTM E3-80 standard, metallographic equipment, Nitral 4% and an attack time 15s.

4.4. Measurement of surface microhardness

In order to study surface hardness variation caused by HEDG conditions, a Vickers microhardness sweep (Buheler-4046 tester) was employed in a cross section of the workpiece. The applied force for microhardness measurement was 100gf for 15s. The indentations were made with a 0.5 mm distance in the cross section of the workpieces, covering the entire surface (i.e., from one side to the other side of the workpiece). Three different indentations were made for each distance to get an average microhardness value. The average was calculated by neglecting the values that are significantly outside the range demarcated by the other measures. If the measures are outside but close to the range, the indentations continue until a representative amount is achieved.

4.5. Measurement of HEDG temperature

Recording of temperature values were essential for analyzing the hardness variations in the samples more precisely. The temperature values were recorded by means of an Infrared/Type K Thermometer (TES-1327K) as shown in Figure 2. The temperature acquired corresponding to the optimized state was approximately recorded 496°C.

4.6. Measurement of HEDG forces

Monitoring of grinding forces is essential because the amounts of forces should not exceed a reasonable range. A dynamometer (Kistler B9255) with amplifier (Kistler A5070) was employed for controlling the forces in the HEDG process. During the process, all force values were recorded for tangential, normal and horizontal forces in the X-axis, Y-axis and Z-axis directions respectively.

4.7. Measurement of surface roughness

As mentioned before, it should be noted that the optimization of one parameter like hardness must not have any unpleasant influence on the other properties. Thus, surface roughness and superficial properties have to be controlled by adjusting cutting parameters of the grinding process. Therefore, in this work the roughness values were measured after finishing grinding of each sample. The obtained values acquired by a Profilometer (Taylor Hobson Surtrunic 25) were within an acceptable range.

5. Results and Discussion

5.1. Optimization of operating process parameters

The parameters obtained by considering the optimization conditions are given in Table 2 and Figure 3 depicts the optimized values resulted from SA algorithm, in terms of iteration. It should be noted that the parameters and constraints should not exceed the allowance limits during the optimization procedure. The optimized state was tested three times. The optimized values for the parameters were $a_e = 1.16$, $v_w = 26.88$, $s = 5.66$ and $v_c = 105$.

Applying the obtained optimized parameters, the values of other sub-objects like hardness, temperature, forces and roughness could be obtainable. These values were measured experimentally and compared with the theoretical values. As it is obvious in Table 3, no considerable deviation was observed between the real and obtained values.

Table 1. Nominal chemical composition and mechanical properties of AISI1045 Steel (wt.%)

C	Si	Fe	Mn	P	S	Cr
0.43-0.50	0.25	98.51 - 98.98	0.60-0.90	≤ 0.04	≤ 0.05	≤ 0.2

Modulus of elasticity	Density	Thermal expansion(20ºC)	Specific heat capacity	Tensile strength	Poisson's Ratio	Thermal conductivity	Yield strength
201 GPa	7.872*10³kg/m³	15.1*10^{-6} ºC^{-1}	486J/(kg*K)	585 MPa	0.290	50.9W/(m*K)	505 MPa

Table 2. The optimized values are acquired by each function and the total optimized values which satisfy each four sub-objective functions have been given.

Repetition number of solutions / Functions	First solution set $\begin{bmatrix} v_w(\frac{m}{min}) & v_c(\frac{m}{s}) \\ s(\frac{mm}{Pass}) & a_e(mm) \end{bmatrix}$	Second solution set $\begin{bmatrix} v_w(\frac{m}{min}) & v_c(\frac{m}{s}) \\ s(\frac{mm}{Pass}) & a_e(mm) \end{bmatrix}$	Third solution set $\begin{bmatrix} v_w(\frac{m}{min}) & v_c(\frac{m}{s}) \\ s(\frac{mm}{Pass}) & a_e(mm) \end{bmatrix}$
Hardness sub-objective function	$\begin{bmatrix} 25.12 & 110 \\ 11.12 & 1.48 \end{bmatrix}$	$\begin{bmatrix} 25.45 & 110 \\ 11.21 & 1.49 \end{bmatrix}$	$\begin{bmatrix} 25.91 & 110 \\ 11.11 & 1.51 \end{bmatrix}$
Heat loading sub-objective function	$\begin{bmatrix} 20.36 & 95 \\ 3.00 & 0.99 \end{bmatrix}$	$\begin{bmatrix} 20.56 & 95 \\ 3.00 & 0.90 \end{bmatrix}$	$\begin{bmatrix} 19.48 & 95 \\ 3.00 & 1.08 \end{bmatrix}$
Mechanical laoding sub-objective function	$\begin{bmatrix} 15.23 & 80 \\ 4.00 & 1.31 \end{bmatrix}$	$\begin{bmatrix} 16.45 & 80 \\ 4.00 & 1.35 \end{bmatrix}$	$\begin{bmatrix} 16.02 & 80 \\ 4.00 & 1.34 \end{bmatrix}$
Roughness sub-objective function	$\begin{bmatrix} 6.01 & 41 \\ 2.00 & 0.2 \end{bmatrix}$	$\begin{bmatrix} 6.36 & 41 \\ 2.00 & 0.79 \end{bmatrix}$	$\begin{bmatrix} 5.98 & 41 \\ 2.00 & 0.71 \end{bmatrix}$
Total objective function	$\begin{bmatrix} 26.88 & 105 \\ 5.51 & 1.17 \end{bmatrix}$	$\begin{bmatrix} 27.69 & 105 \\ 5.64 & 1.16 \end{bmatrix}$	$\begin{bmatrix} 26.88 & 105 \\ 5.66 & 1.16 \end{bmatrix}$

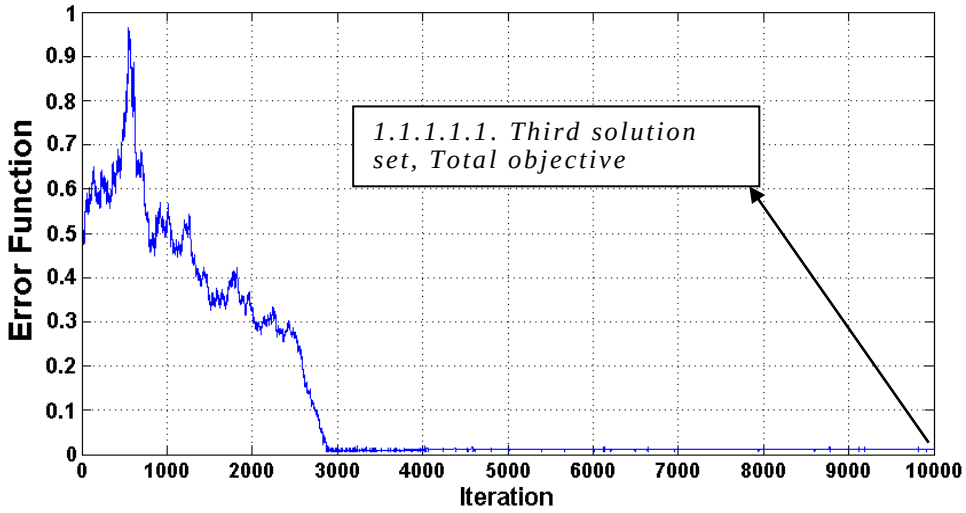

Fig. 3 Total objective function graph and parameters related to the optimized conditio

Table 3. The experimental and theoretical values corresponding to the optimized condition

Values / Object	HB	T_{max} (°C)	F' (N/mm)	R_t (μm)
Real values	273	496	91.4	1.1
Obtained values from optimization	270	487	88.6	1.0

Table 4. The measured values of Vickers microhardness before (A) and after (B) process

	First Vickers Value	Second Vickers Value	Third Vickers Value	Fourth Vickers Value	Fifth Vickers Value	Average Vickers Value	Brinell Hardness	Rockwell Hardness HRB	Rockwell Hardness HRC
State A	179	183	187	175	179	180.6	172	87	-
State B	289	292	285	282	282	286	273	-	28

5.2. Metallographic and hardness analysis

For the evaluated conditions, metallographic analysis of the hardness values leaded to the following conclusions. Although occurrence of some changes in microstructure of the samples was prospected, microstructural changes before and after the process were insignificant even for those samples subjected to an excess heat. The surface microhardness was recorded five times before and after HEDG process and as illustrated in Table 4, a considerable increase was observed in superficial microhardness.

Fig. 4 The optical micrographs of polished surface of samples illustrating Ferrite and Perlite at AISI1045 steel, (A) before the HEDG process, (B) after the process under the total optimized condition mentioned in Table 2

The previous researchers have revealed that the residual stress as a representative of the hardness is originally induced by the following procedures [14]:

i. Martensite transformation below the surface

ii. Plastic flow of the material on the surface and the adjacent zones as a result of thermal stresses which are caused by heat generation during the operation

iii. Plastic deformation at the workpiece surface due to the forces of abrasive grits.

Plastic deformation beneath the surface is generated by parameters of grinding, such as grit size, workpiece speed, depth of cut and material properties. As the used steel has low hardenability and on the other hand, the TTT diagram of AISI1045 steel shows that the cooling curve for the martensitic transformation must be almost vertical because of the low percentage of carbon as well as the absence of other chemical elements in this alloy. In other words, this alloy should be cooled very quickly in order to reach a martensitic microstructure. The cooling rate applied in this study was not sufficient to lead to this transformation. Moreover, the temperature was measured by Infrared Thermometer during the operations and the maximum amount of temperature was recorded at 496°C. This value of temperature could unlikely be associated with any plastic flow and microstructural transformation in the samples. This conclusion was validated by the ferritic-pearlitic microstructure of the samples, illustrated in Figure 4 and was related to the annealing heat treatment of the workpiece which was ground under the global optimization condition. In fact, the grinding process produces fine and equiaxed grains in structure of materials, Figure 4. Accordingly, as the microstructural transformations and plastic flow of the material were inconsiderable, hardness enhancement was the result of the finer microstructure achieved and a sever plastic deformation induced by material removal process in the workpiece [15].

As Figure 5 shows, the microhardnesses measurement within a specific section of the workpiece demonstrated a significant increase as the depth of measurement decreases. This change was due to the intensive machining heat and then sever cooling rate at the surface of the workpiece as well as the sever plastic deformation. The plastic deformation beneath the surface is corresponded to HEDG's parameters. Moreover, according to the previous studies [16, 17], hardness enhancement is also associated with the parameters of HEDG process because plastic deformation beneath the surface is directly corresponded to these parameters i.e. cross feed, depth of cut, wheel speed and worktable speed. In other words, the higher values of these parameters implicates an increase in cutting area and consequently cutting force which results in the increase of the material removing and the plastic deformation as well as the hardness of the workpiece surface. As a result, the hardness of the workpiece's surface was increased significantly. These events resulted in the compressive residual stress in materials that is consistent with previous investigations [18]. However, as the values of these parameters decrease, the amount of work for the same quantity of grains decreases. This leads to reduction of the pressure between the wheel and the workpiece, the cutting force and the traction generated by slipping of the grains across the surface as well as lower friction and heat generation. Consequently, as it is obvious in Figure 5, at lower values of HEDG parameters the surface hardness of the samples was increased, but not to its maximum value.

It has been proved that tensile and compressive residual stresses are produced by thermal loads and high mechanical loads of the grinding process [19]. It means that the operating parameters leading to high temperatures within the contact zone induce residual tensile stresses, while the operating parameters which result in high mechanical loads induce compressive residual stress in the workpiece. Reducing of the friction force, typically results in reducing heat generation in contact zone. Creep feed grinding reacts to increase in depth of cut more than the ground parts by reciprocating grinding, as it leads to transfer the residual stress to compressive zone in different studied situation. Thus, when the specific removal rate $Q'_w = a_e.\mathrm{v}_w$ is increased the compressive residual stresses are increased. This event can be elucidated by increasing of the workpiece speed which causes that the heat load has no enough time to penetrate to the workpiece. In other words, the residual tensile stresses that are induced by thermal load are compensated by the excessive compressive residual stress induced mechanically. As well as, the higher wheel speed results in increasing hardness and compressive residual stress. In fact, at a higher wheel speed the contact layer which is temporarily hot, is removed immediately

and consequently the lower temperature could penetrate to the workpiece.

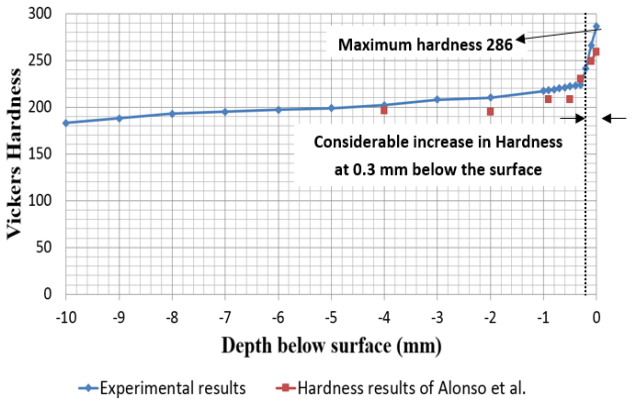

Fig. 5 The graph of microhardness below the surface under optimized condition obtained by experiment compared with Alonso's results

Figure 5 shows the measured microhardness values in a cross section of the workpiece and perpendicular to the grinding direction. These values were measured three times in each 1mm at the cross section, incidentally this measurement was performed in each 0.1mm upon the first 1mm of the cross section. The maximum microhardness was recorded 286HV that was corresponded to the top surface. As it can be seen, the microhardness values beneath the surface is higher than in depth. A similar study has been done by Alonso et al. to investigate the effects of grinding parameters on the surface hardening of AISI1045 [20]. In their work, three parameters namely depth of cut, cross feed and infeed have been considered as process parameters. They reached to this conclusion that by increasing the above-mentioned parameters, the surface hardness of ground specimens can be improved. Figure 5 compares their results with the results of present study. Based on their results, it can be claimed that the more the parameters of grinding process, the harder the surface of specimens. However, it should be borne in mind that increasing the surface hardness of materials can bring about some destructive side effects. That is, the surface roughness of material can be deteriorated by increasing the process parameters. On the other hand, the surface roughness or thermal damages due to elevated temperature may become worsen if it is supposed to access a higher hardness. Therefore, a strong need for optimization of grinding process is felt to attain a desirable result. The present study attempted to fulfill this need by implementing the SA optimization method to reach a combination of desired parameters. comparing the obtained results of optimization approach with Alonso's experiments, it can be observed that the optimization's results of this study regarding to the surface hardness is relatively similar to Alonso's results [20].

The measured values R_t were ranged from 0.9µm to 1.2µm (R_a = 0.7-0.9µm). The equivalent roughness value corresponded to optimized hardness value (286HV) was 1.1µm. Additionally, during the process, all force values were not exceeded the range of 20-35N/mm, 75-105N/mm and 1.25-1.75N/mm for tangential, normal and horizontal forces respectively. The equivalent total force corresponded to optimized hardness value is 91.4N/mm (X-axis: 32.5N/mm, Y-axis: 85.5N/mm and Z-axis: 1.5N/mm). As a result, a simultaneous control on four aspects of grinding process can result in a high quality product.

6. Concluding remarks

With considering of the outputs of the optimization procedure, overall observations and results related to the hardness, the studies were led to the below points:

1- As the operating parameters were selected highly, the measured hardness was increased.

2- By employing the conditions were concluded by the optimization procedure, the strength and obtained microhardness values increased, thus, the needs for hardening heat treatment were eliminated in industries.

3- Despite the optimization outputs were ended up the parameters that produce compressive residual stress at the surface, the measured roughness value corresponded to the optimal conditions was almost remained in an idealistic range.

4- The LSG conditions were conducted by considering the aspects of the multi-objective optimization and applying the total optimum conditions.

5- SA method was successfully implied to solve the process's problems to robustly diminish the residual tensile stresses. This procedure can be readily modified to suit other metal cutting processes like turning, cylindrical grinding and non-conventional machining operations.

6- One of the advantages of the used simulation is that it could represent systematic tests to investigate the effects of one particular parameter on the results of finish surface.

7- Due to the surface hardness of the workpieces, the fatigue life of materials is increased. These Types of workpieces can be used in dynamic applications.

7. Acknowledgements

The authors gratefully acknowledge helpful and valuable technical suggestions, references suggested and provided by Dr. Arab (Rajaee university of Tehran, Iran) in early phases of this study. The authors are also grateful to the anonymous referees for their valuable comments and suggestions. The authors would also like to thank the financial support from South Pars Gas Company (SPGC) in Bushehr province in funding this research and assistance provided by and Dr.Motakef Imani (CAD/CAM Lab Division), Dr.Babakhani (Metallography Lab Division) and Dr.Sajadi (Heat Treatment Lab Division) of Ferdowsi University of Mashhad.

References

[1] J. J. Martell, C. R. Liu, J. Shi, Experimental investigation on variation of machined residual stresses by turning and grinding of hardened AISI 1053 steel, The International Journal of Advanced Manufacturing Technology, Vol. 74, No. 9-12, pp. 1381-1392, 2014.

[2] O. Fergani, Y. Shao, I. Lazoglu, S. Y. Liang, Temperature effects on grinding residual stress, Procedia CIRP, Vol. 14, pp. 2-6, 2014.

[3] Y. Deng, S. Xiu, Research on microstructure evolution of austenitization in grinding hardening by cellular automata simulation and experiment, The International Journal of Advanced Manufacturing Technology, pp. 1-14, 2017.

[4] C. Yao, T. Wang, J. Ren, W. Xiao, A comparative study of residual stress and affected layer in Aermet100 steel grinding with alumina and cBN wheels, The International Journal of Advanced Manufacturing Technology, Vol. 74, No. 1-4, pp. 125-137, 2014.

[5] Y. Xiao, A. Konak, A simulating annealing algorithm to solve the green vehicle routing & scheduling problem with hierarchical objectives and weighted tardiness, Applied Soft Computing, Vol. 34, pp. 372-388, 2015.

[6] C. A. Floudas, P. M. Pardalos, 2014, Recent advances in global optimization, princeton University press,

[7] S.-m. Ahn, S.-Y. Park, Y.-C. Kim, K.-S. Lee, J.-Y. Kim, Surface residual stress in soda-lime glass evaluated using instrumented spherical indentation testing, Journal of materials science, Vol. 50, No. 23, pp. 7752-7759, 2015.

[8] K. Deb, Multi-objective optimization, in: Search methodologies, Eds., pp. 403-449: Springer, 2014.

[9] M. Azadi Moghaddam, F. Kolahan, An empirical study on statistical analysis and optimization of EDM process parameters for inconel 718 super alloy using D-optimal approach and genetic algorithm, Journal of Computational Applied Mechanics, Vol. 46, No. 2, pp. 267-277, 2015.

[10] K. Salonitis, A. Kolios, Experimental and numerical study of grind-hardening-induced residual stresses on AISI 1045 Steel, International Journal of Advanced Manufacturing Technology, Vol. 79, 2015.

[11] A. D. Batako, M. Morgan, B. W. Rowe, High efficiency deep grinding with very high removal rates, The International Journal of Advanced Manufacturing Technology, Vol. 66, No. 9-12, pp. 1367-1377, 2013.

[12] W. B. Rowe, 2013, Principles of modern grinding technology, William Andrew,

[13] G. Khalaj, H. Yoozbashizadeh, A. Khodabandeh, A. Nazari, Artificial neural network to predict the effect of heat treatments on Vickers microhardness of low-carbon Nb microalloyed steels, Neural Computing and Applications, Vol. 22, No. 5, pp. 879-888, 2013.

[14] A. Bayat, R. Moharami, Numerical Analysis of explosion effects on the redistribution of residual stresses in the underwater welded pipe, Journal of Computational Applied Mechanics, Vol. 47, No. 1, pp. 121-128, 2016.

[15] Y. Zhang, X. J. Meng, Z. J. Yuan, Study of Grinding Hardening Force Based on the Influence of Grinding Arc Temperature and Workpiece Deformation, in Proceeding of, Trans Tech Publ, pp. 98-103.

[16] Y. Shao, O. Fergani, Z. Ding, B. Li, S. Y. Liang, Experimental investigation of residual stress in minimum quantity lubrication grinding of AISI 1018 steel, Journal of Manufacturing Science and Engineering, Vol. 138, No. 1, pp. 011009, 2016.

[17] M. Hamedi, H. Eisazadeh, Numerical Simulation of Nugget Geometry and Temperature Distribution in Resistance Spot Welding, Journal of Computational Applied Mechanics, Vol. 46, No. 1, pp. 13-19, 2015.

[18] K. Salonitis, On surface grind hardening induced residual stresses, Procedia CIRP, Vol. 13, pp. 264-269, 2014.

[19] U. Alonso, N. Ortega, J. A. Sanchez, I. Pombo, S. Plaza, B. Izquierdo, In-process prediction of the hardened layer in cylindrical traverse grind-hardening, The International Journal of Advanced Manufacturing Technology, Vol. 71, No. 1-4, pp. 101-108, 2014.

[20] U. Alonso, N. Ortega, J. Sanchez, I. Pombo, B. Izquierdo, S. Plaza, Hardness control of grind-hardening and finishing grinding by means of area-based specific energy, International Journal of Machine Tools and Manufacture, Vol. 88, pp. 24-33, 2015.